nature structural & molecular biology

Myosin VI walks hand-over-hand along actin

Zeynep Ökten[1,2], L Stirling Churchman[1,3], Ronald S Rock[1] & James A Spudich[1]

Myosin VI is a molecular motor that can walk processively on actin filaments with a 36-nm step size. The walking mechanism of myosin VI is controversial because it takes very large steps without an apparent lever arm of required length. Therefore, myosin VI is argued to be the first exception to the widely established lever arm theory. It is therefore critical to directly demonstrate whether this motor walks hand-over-hand along actin despite its short lever arm. Here, we follow the displacement of a single myosin VI head during the stepping process. A single head is displaced 72 nm during stepping, whereas the center of mass previously has been shown to move 36 nm. The most likely explanation for this result is a hand-over-hand walking mechanism. We hypothesize the existence of a flexible element that would allow the motor to bridge the observed 72-nm distance.

Myosin VI is an actin-based molecular motor that is ubiquitously expressed in higher organisms. Myosin VI is thought to be involved in a variety of cellular functions. For example, it has been proposed to be involved in endocytosis in epithelial cells by transporting uncoated or clathrin-coated vesicles toward the early endosome through a dense actin meshwork[1,2]. At the cell cortex, polarized actin filaments are anchored with their barbed ends at the plasma membrane and their pointed ends facing the cell interior. Whereas myosin II and V move toward the barbed end of an actin filament, myosin VI moves toward the pointed end[3], which would allow it to carry out the suggested role in endocytosis. In Snell's waltzer mice, a defective myosin VI leads to deafness and loss of coordination, apparently by disturbing the structural integrity of stereocilia in cochlear hair cells[4,5]. In this role, myosin VI seems to act as an anchor, stabilizing the tension needed in the stereocilia. Recent data show that myosin VI can act as an anchor or as a dynamic tension sensor in cells by strain-dependent alteration of the rate of ADP binding to the motor[6].

The N-terminal part of myosin VI is a typical catalytic domain that binds actin and nucleotide. Just C-terminal to the catalytic domain is a light chain binding domain that constitutes a putative lever arm. This light chain binding domain is adjacent to a tail domain, part of which is strongly predicted to be a coiled coil. The coiled-coil region is probably involved in creating a functional dimeric motor. Notably, the full-length myosin VI from chicken intestinal brush border has been found to be a monomer[7], and it seems likely that the dimerization state of myosin VI might be regulated *in vivo* in a manner that remains to be elucidated.

According to the lever arm model, the step size of myosins is predicted to be proportional to their length of the lever arm, which is the light chain binding region. A great deal of evidence supports the hypothesis, for example, that myosin V uses its light chain binding domains as a long lever arm. Each myosin V lever arm binds six light chains to step 36 nm hand-over-hand along an actin filament[8–14]. Recent experiments[13,14] have conclusively demonstrated such hand-over-hand stepping of myosin V. The mechanism of movement of myosin VI, on the other hand, seems to be considerably more complex and not fully explained by a lever arm mechanism. Myosin VI has only two light chains in each of its lever arms[15], but it processively moves with a large step size of ~30 ± 12 nm when measured against a load of 1.7 pN (ref. 12). At low loads, the step size increases to ~36 nm (ref. 6). These step sizes are much larger than expected for a lever arm consisting of only two calmodulin light chains. The discovery of a myosin with a short lever arm but a large step size has led to controversial proposals for the working mechanisms of myosin VI[12,16].

A modification of the lever arm model has been proposed that predicts a step consisting of a working stroke of the short lever arm followed by a diffusive search[12]. The working stroke provides part of the step size and imparts directionality while the diffusive search allows the leading head to find further actin-binding sites. This proposal predicts that elements of the myosin VI protein may become flexible during periods of the stepping cycle, which extends the reach of the myosin VI heads and allows larger step sizes.

The proposed flexible element could be in the tail domain, C-terminal to the light chain binding region. The proximal tail domain is an attractive candidate as it has a low propensity to form a coiled coil[6,17]. A flexible element could also derive, however, from some part of the structure N-terminal to the IQ domain that binds calmodulin. The unique insert had been considered as a domain that might unfold to provide this flexibility, but the recent discovery that the unique insert binds calmodulin in a structurally permanent manner argues against a possible unfolding of the unique insert[15].

Given the complexity of myosin VI, a direct measurement of whether hand-over-hand movement occurs in this case would be particularly valuable to further our understanding of how this unusual

[1]Stanford University School of Medicine, Beckman Center, 279 Campus Drive, Stanford, California 94305-5307, USA. [2]Department of Biology, Chemistry and Pharmacy, Freie Universität Berlin, Taku Strasse 3, Institut für Chemie, Berlin 14195, Germany. [3]Department of Physics, 382 Via Pueblo Mall, Stanford University, Stanford, California 94305-4060, USA. Correspondence should be addressed to J.A.S. (jspudich@stanford.edu).

Published online 1 August 2004; doi:10.1038/nsmb815

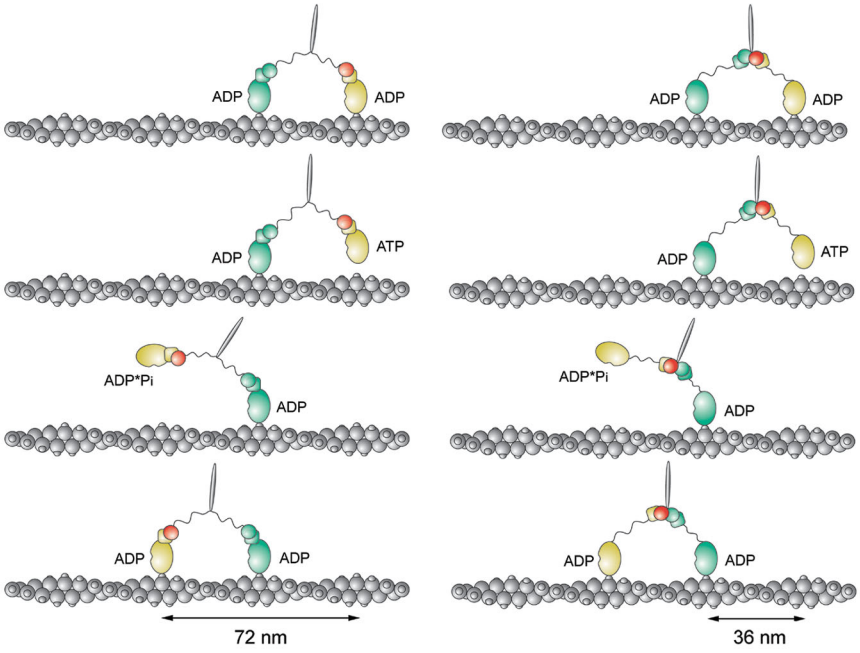

Figure 1 Proposed hand-over-hand mechanism for myosin VI. Left panel, a myosin VI molecule walking to the left with its putative flexible element C-terminal to the labeled calmodulin. A fluorescent label attached to one calmodulin (red) moves ~72 nm associated with one ATP hydrolysis. Thus, the trailing head (yellow) becomes the new leading head. The next ATP hydrolysis does not alter the fluorophore position and results in a 0-nm step. Right panel, a molecule walking to the left with its putative flexible element N-terminal to the labeled calmodulin. In this model, with each ATP hydrolysis, the fluorophore (red) moves ~36 nm.

motor works. Here we report that this motor does indeed walk hand-over-hand along actin.

RESULTS

Proposed stepping models of myosin VI

To elucidate the myosin VI stepping mechanism, we probed with nanometer resolution fluorescently labeled single molecules of myosin VI walking on actin filaments. If only one neck of myosin VI is dye labeled, the observed dye movement provides valuable information about the stepping mechanism. According to a hand-over-hand model, the heads swap orientation during the stepping cycles, resulting in an alternation of the leading positions. After each ATP hydrolysis, the trailing head becomes the new leading head (**Fig. 1**). The figure shows two stepping models of a myosin VI molecule labeled with a single Cy5 fluorophore on one calmodulin, indicated in red. In the left panel, the putative flexible element is C-terminal to the labeled calmodulin, and results in a ~72-nm displacement of the fluorophore. In the right panel, the putative flexible element is N-terminal to the labeled calmodulin, and results in a ~36-nm displacement of the fluorophore. An alternative to hand-over-hand walking is the inchworm model, which involves one head always serving as the leading head with the trailing head being pulled up from behind at each step (**Supplementary Fig. 1** online). Thus, according to this model, throughout the stepping cycles, the trailing head is dragged after the leading head with each ATP hydrolysis. According to the inchworm model, the fluorophore would be displaced ~36 nm regardless of where the putative flexible element is.

Calmodulin labeling in the wild-type background of myosin VI

We used total internal reflection fluorescence (TIRF) microscopy to observe Cy5 labeled myosin VI molecules. The fluorescent label was attached to an engineered cysteine that was inserted into the native cysteine-free calmodulin light chain of myosin VI. To attain labeling specificity over the 22 native cysteines in one heavy chain of the myosin VI construct, we N-terminally tagged the calmodulin light chain with Lys-Lys-Cys-Lys and coexpressed it with the myosin heavy chain in SF9 cells. The high p*K*a of the lysines makes the mutant cysteine more nucleophilic compared with the native cysteines, allowing specificity for the labeling reaction[18]. Myosin VI expressed together with the N-terminally tagged calmodulin exhibited identical properties in *in vitro* motility assays compared with the wild-type protein (data not shown).

The cysteine-tagged protein was reacted with Cy5 at a 1:1 molar ratio. At this molar ratio, 10–15% of available sites reacted with Cy5 as determined in titration experiments (**Supplementary Fig. 2** online). The labeling was ~90% specific, as judged by the ratio of the heavy chain fluorescence to the light chain fluorescence in a fluorescence scan of an SDS-polyacrylamide gel (**Supplementary Fig. 3** online).

Myosin VI walks processively on suspended filaments

The lack of processivity of myosin VI on entirely surface-attached filaments has hampered investigations of this motor protein in single-molecule TIRF experiments. This lack of processivity is presumably due to protein-surface interactions. To overcome this problem, we suspended actin filaments in solution by draping them between spherical beads (90-nm diameter) that sparsely coat the cover slip. The actin filaments were biotin-labeled, allowing them to adhere firmly to the streptavidin-coated spherical beads. This geometry provides for long stretches of actin that are raised off the surface of the slide but are still within the total internal reflection excitation zone of the microscope. We showed that myosin VI can processively walk on these actin

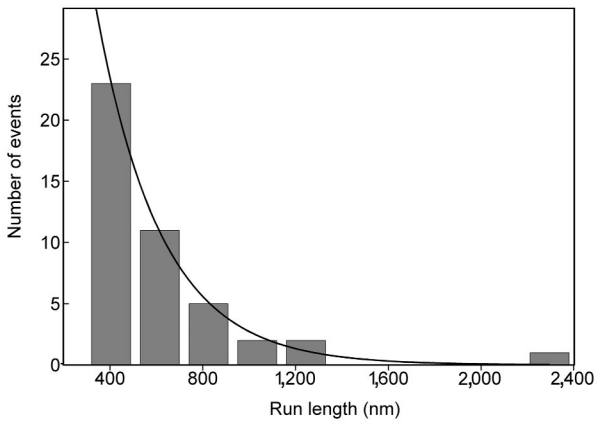

Figure 2 Run-length distribution of single fluorescently labeled myosin VI molecules in the single molecule assays. Myosin VI walks processively on the suspended actin filaments with an average run length of 280 nm ($n = 43$). Run lengths ≥300 nm were tabulated and fit to a single exponential.

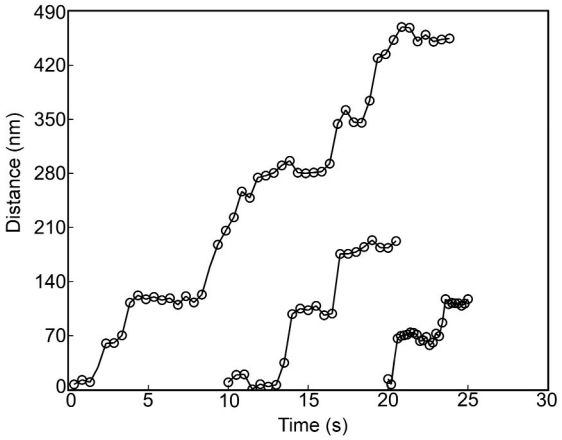

Figure 3 Staircases of three different fluorescently labeled myosin VI molecules. These staircases show the processive stepping of myosin VI on actin filaments. The integration time is 0.5 s for all staircases with an ATP concentration of 40 μM.

filaments with an average run length of 280 nm ($n = 43$) (**Fig. 2**)[19], and it can walk distances up to 2.4 μm on fully suspended filaments. These measured run lengths are probably underestimated because the protein can walk in or out of the evanescent field or the dye can photobleach while the myosin still walks along the actin.

The suspended actin filaments are far enough from the surface to support long run lengths, but motors on these filaments appear dim and are not generally suitable for a precise step-size determination (**Supplementary Videos 1** and **2** online).

Single fluorophores were localized with high resolution

To measure the displacement of the labeled motor, we localized its single Cy5 to within 1 nm. Circumventing the diffraction limit by fitting the fluorescent peak to a two-dimensional Gaussian has been used to analyze the stepping of myosin V and kinesin[14,20]. A sample Cy5 single fluorophore localization (SFL) using the same approach is shown in **Supplementary Figure 4** online. The two-dimensional Gaussian fit to this peak yielded a σ_μ of 0.19 nm. A bootstrap analysis was carried out to further analyze the error on the SFL. The point spread function (PSF) was turned into a distribution of pixel values, each with a frequency of the pixel's intensity. From this distribution of size N, 200 bootstrap distributions of size N were made. Fitting the 200 bootstrap PSFs to the two-dimensional Gaussian yielded 200 center locations, which by the central limit theorem is normally distributed; the variance is the standard error of the center's location. The s.d. of bootstrap PSF's locations was 0.39 nm. This is a model-independent confirmation that the fluorophores were fit to within 1 nm.

Furthermore, the low ATP concentration (3 μM) used for the sample fluorophore allowed us to image it multiple times bound to the same actin monomer for 10 s (**Supplementary Fig. 4** online). The spot's fluorescence dropped to background in a single step, suggesting that the Cy5 either photobleached or the motor detached after this time. The ten localizations resulted in an s.d. of 6.5 nm. A large component of the localization variance is probably due to the flexibility of the actin filaments bridging the beads. Our actin filaments are only secured when they are in contact with a bead; hence, the stretch of filament between beads is loose enough to undergo brownian motion.

As the labeled myosin VI moves along the actin with 40 μM ATP, we see displacement of the Cy5 fluorophore occurring in discrete steps (three examples, **Fig. 3**). We analyzed 85 transitions of 67 individual single fluorescently labeled myosin VI heads under zero load conditions and found that the mean of the step-size distribution is 70 ± 23 nm (**Fig. 4**). The second peak of 165 ± 15 nm on the histogram presumably represents two rapid steps. For the step-size histogram, only motors that were close to the surface of the evanescent field yielded high enough numbers of photons to localize with high resolution. Molecules close to the surface have decreased processivity, and therefore most transitions came from single transitions of myosin VI. Under low loads, myosin VI steps ~36 nm (refs. 6,16), which is half of the fluorophore displacement size in our experiment. These findings are consistent with the hand-over-hand mechanism and the use of a flexible element in the tail domain to extend the reach of the lever arm (**Fig. 1**, left panel). They are not consistent with a flexible element N-terminal to the calmodulin-binding site (**Fig. 1**, right panel), or an inchworm model (**Supplementary Fig. 1** online).

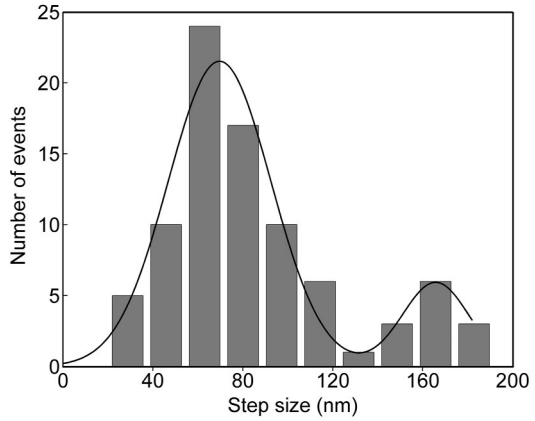

Figure 4 Step-size histogram of single fluorescently labeled myosin VI molecules. The data were fit to a double Gaussian with a mean step-size distribution of 70 ± 23 nm for the main peak and 165 ± 15 nm for the second peak. The second peak presumably represents two rapid steps that are unresolved.

DISCUSSION

We conclude that myosin VI does not have a fundamentally different stepping mechanism than other characterized myosins in the myosin superfamily. As already shown in the optical trapping experiments[12], myosin VI exhibits a broad step-size distribution (**Figs. 3** and **4**), and this probably derives from a diffusive flexible element, which, as we show here, would have to derive from the tail domain. The stepping mechanisms of myosin V and myosin VI seem to differ primarily in their different partial contributions of the power stroke and the diffusive search to the step size. Myosin V stepping is determined largely by a power stroke with a smaller contribution of a diffusive search, leading to a narrow step-size distribution[21,22]. Myosin VI stepping, on the other hand, is largely determined by a diffusive search, leading to a broad step-size distribution. The power stroke, recently measured to be ~12–18 nm (ref. 7) (R.S.R. and A. Dunn, Stanford University, unpublished results), presumably biases the leading head and determines the direction of movement.

METHODS

Protein expression and purification. The following plasmid, a gift of H. Lee Sweeney, University of Pennsylvania, was the starting point for our construct. The plasmid codes for porcine myosin VI that is truncated at Ala990 to create a

double-headed myosin VI construct including 20 native heptad repeats of the predicted coiled coil. To ensure dimerization, a leucine zipper (GCN4) was added at the C-terminal end of the native coiled coil. The leucine zipper was followed by YFP and a Flag-tag (GDYKDDDDK) to facilitate purification.

We used this plasmid to introduce a modified calmodulin with a sequence containing a highly reactive cysteine residue (KKCK). A dual expression vector, p2Bac/pFastBac-MyoVI-CaM, was created for recombinant baculovirus generation. For the mutagenesis, the wild-type gene encoding CaM was subcloned into the p2Bac/pFastBac vector to give p2Bac/pFastBac-CaM. This vector was PCR-amplified using primers that contained the in-frame fusions of the KKCK coding tag. The PCR product was cloned into p2Bac/pFastBac to create the mutant CaM containing p2Bac/pFastBac-CaM^{m}. To create the dual expression vector p2Bac/pFastBac-CaM^{m}-Myo VI, the wild-type gene encoding myosin VI was cloned into the p2Bac/pfastBac-CaM^{m} vector. The resulting vector contained the mutagenized gene encoding CaM under the p10 promoter and the gene encoding wild-type myosin VI under the polyhedrin promoter, respectively. The generation of recombinant baculovirus protein expression in SF9 cells and purification were pursued as described[23]. The recombinant protein was labeled at 23 °C with Cy5 in a molar ratio of 1:1 Cy5 to myosin VI immediately after the elution from the Flag column. The reaction was quenched with 10 mM DTT after 20 min. To separate unreacted dye from the protein, the reaction mixture was purified over a MonoS column. The protein-containing fractions were pooled and dialyzed into the *in vitro* motility assay buffer containing 25 mM KCl, 25 mM imidazole HCl, pH 7.4, 1 mM EGTA, 4 mM $MgCl_2$ and 10 mM DTT. In addition, 50% (v/v) glycerol was added to the assay buffer for storage purposes.

Motility assays. All single molecule motility assays were carried out in the motility buffer, which is assay buffer including 4.5 μM purified wild-type CaM at 23 °C, and the following additional components. To reduce photobleaching, an oxygen scavenging system (11 μg ml^{-1} glucose oxidase, 18 μg ml^{-1} catalase, 0.23% (w/v) glucose and 0.13% (v/v) β-mercaptoethanol) was added along with an ATP regeneration system (0.1 mg ml^{-1} creatine phosphokinase, 1 mM creatine phosphate) in the motility buffer. To reduce nonspecific background binding of myosin VI, 1% (v/v) Triton-X 100 and 1 mg ml^{-1} BSA were included in the motility buffer. The single molecule motility experiments were carried out in 40 μM ATP and with 300 pM motor protein.

All gliding filament *in vitro* motility assays were done as described with 2 mM ATP except with 22 μg ml^{-1} glucose oxidase, 36 μg ml^{-1} catalase, 0.45% (w/v) glucose and 0.25% (v/v) β-mercaptoethanol[24].

Suspension of actin filaments and flow cell preparation. A dilution of 1:150 of streptavidin-coated, spherical polystyrene beads of 90-nm diameter (Bangs Laboratories) in assay buffer was used to prepare a flow cell with suspended actin filaments. The coverslip was coated with 1 mg ml^{-1} biotin-BSA and sparsely covered with the diluted streptavidin beads. The surface was then blocked with additional 1 mg ml^{-1} BSA in assay buffer. Biotinylated TRITC phalloidin actin filaments (excitation, 557 nm; emission, 576 nm) at a final concentration of 100 nM were flowed in, followed by the motility buffer containing the motor protein. An incubation time of 2 min was allowed between each step.

Microscope setup. Excitation source beams at 532 nm (Coherent) and 633 nm (JDS Uniphase) were combined by a dichroic mirror, and expanded to 7-mm diameter. These sources were focused (focal length = 500 mm) on the back focal plane of an Olympus 1.65 NA 100X TIRF objective, via a laser line dichroic on a linear translation stage that allows microscope operation in either epifluorescence or TIRF modes. The reflected light exiting the back aperture of the objective was directed on a quadrant photodiode to provide a signal for a focus feedback loop that clamped the distance between the objective and sample using an electrostrictive actuator (Newport). Fluorescence emission was collected by the objective and passed through a dual-view apparatus that allowed simultaneous imaging of the Cy5 and TMR channels on a single EMCCD camera. Data were collected with the Andor iXon DV887 and Roper Cascade 512B camera. The two step-size data sets collected with these cameras are statistically indistinguishable by a *t*-test ($t(54, 31) = 0.1$, $P > 0.05$).

Single fluorophore localization. To localize the fluorophores, we fit the peaks to two-dimensional Gaussians (**Supplementary Fig. 4** online). The myosin VI stepping experiments were done at several integration times (0.5 s, 0.3 s, 0.2 s). The power of the excitation laser was adjusted for each integration time such that the fits yielded the same localization precision. The pixel size of our images was determined by translating in two orthogonal directions a 1.0-μm TransFluoSpheres bead (Molecular Probes) in 500-nm steps, creating a grid of fiducials. These beads emit light at ~543 nm and 620 nm, allowing us to detect them in both color channels. A local weighted mean mapping of the fiducials locations (found by a two-dimensional Gaussian fit) to real space was used to calculate an average pixel size. The channel-to-channel mapping was done in a similar manner with the same data set. This allowed us to confirm that the motors we analyzed were colocalized with actin filaments.

Note: Supplementary information is available on the Nature Structural & Molecular Biology website.

ACKNOWLEDGMENTS

We thank B. Spink for assistance in the creation of the construct and H.L. Sweeney for providing the plasmid for myosin VI expression. We thank F. Müller-Planitz for assistance in MatLab programming, helpful discussions and comments on the manuscript. We also thank D.A. Altman and A. Dunn for helpful discussions and comments on the manuscript. This work was supported by Boehringer Ingelheim Fonds to Z.Ö., US National Institutes of Health grant GM33289 to J.A.S. and a Burroughs Wellcome Career Award at the Scientific Interface to R.S.R.

COMPETING INTERESTS STATEMENT

The authors declare that they have no competing financial interests.

Received 4 June; accepted 30 June 2004
Published online at http://www.nature.com/nsmb/

1. Aschenbrenner, L., Lee, T. & Hasson, T. Myo6 facilitates the translocation of endocytic vesicles from cell peripheries. *Mol. Biol. Cell* **14**, 2728–2743 (2003).
2. Buss, F. *et al.* Myosin VI, a new force in clathrin mediated endocytosis. *FEBS Lett.* **508**, 295–299 (2001).
3. Wells, A.L. *et al.* Myosin VI is an actin-based motor that moves backwards. *Nature* **401**, 505–508 (1999).
4. Avraham, K.B. *et al.* The mouse Snell's waltzer deafness gene encodes an unconventional myosin. *Nat. Genet.* **11**, 369–375 (1995).
5. Cramer, L.P. Myosin VI: roles for a minus end-directed actin motor in cells. *J. Cell Biol.* **150**, F121–126 (2000).
6. Altman, D., Sweeney, H.L. & Spudich, J.A. The mechanism of myosin VI translocation and its load-induced anchoring. *Cell* **116**, 737–749 (2004).
7. Lister, I. *et al.* A monomeric myosin VI with a large working stroke. *EMBO J.* **23**, 1729–1738 (2004).
8. Purcell, T.J., Morris, C., Spudich, J.A. & Sweeney, H.L. Role of the lever arm in the processive stepping of myosin V. *Proc. Natl. Acad. Sci. USA* **99**, 14159–14164 (2002).
9. Rief, M. *et al.* Myosin-V stepping kinetics: a molecular model for processivity. *Proc. Natl. Acad. Sci. USA* **97**, 9482–9486 (2000).
10. Spudich, J.A. The myosin swinging cross-bridge model. *Nat. Rev. Mol. Cell Biol.* **2**, 387–392 (2001).
11. Spudich, J.A. How molecular motors work. *Nature* **372**, 515–518 (1994).
12. Rock, R.S. *et al.* Myosin VI is a processive motor with a large step size. *Proc. Natl. Acad. Sci. USA* **98**, 13655–13659 (2001).
13. Forkey, J.N., Quinlan, M.E., Shaw, M.A., Corrie, J.E. & Goldman, Y.E. Three-dimensional structural dynamics of myosin V by single-molecule fluorescence polarization. *Nature* **422**, 399–404 (2003).
14. Yildiz, A. *et al.* Myosin V walks hand-over-hand: single fluorophore imaging with 1.5-nm localization. *Science* **300**, 2061–2065 (2003).
15. Bahloul, A. *et al.* The unique insert in myosin VI is a structural calcium-calmodulin binding site. *Proc. Natl. Acad. Sci. USA* **101**, 4787–4792 (2004).
16. Nishikawa, S. *et al.* Class VI myosin moves processively along actin filaments backward with large steps. *Biochem. Biophys. Res. Commun.* **290**, 311–317 (2002).
17. Berger, B. *et al.* Predicting coiled coils by use of pairwise residue correlations. *Proc. Natl. Acad. Sci. USA* **92**, 8259–8263 (1995).
18. Rice, S. A Structural Change in the Neck Region of Kinesin Motors Drives Unidirectional Motility. Thesis, Univ. of California San Francisco (2001).
19. De La Cruz, E.M., Ostap, E.M. & Sweeney, H.L. Kinetic mechanism and regulation of myosin VI. *J. Biol. Chem.* **276**, 32373–32381 (2001).
20. Yildiz, A., Tomishige, M., Vale, R.D. & Selvin, P.R. Kinesin walks hand-over-hand. *Science* **303**, 676–678 (2004).
21. Veigel, C., Wang, F., Bartoo, M.L., Sellers, J.R. & Molloy, J.E. The gated gait of the processive molecular motor, myosin V. *Nat. Cell Biol.* **4**, 59–65 (2002).
22. Mehta, A.D. *et al.* Myosin-V is a processive actin-based motor. *Nature* **400**, 590–593 (1999).
23. Sweeney, H.L. *et al.* Kinetic tuning of myosin via a flexible loop adjacent to the nucleotide binding pocket. *J. Biol. Chem.* **273**, 6262–6270 (1998).
24. Rock, R.S., Rief, M., Mehta, A.D. & Spudich, J.A. *In vitro* assays of processive myosin motors. *Methods* **22**, 373–381 (2000).